International Journal of Engineering and Advanced Technology (IJEAT)
ISSN: 2249-8958 (Online), Volume-8 Issue-6, August 2019

Regression Examination Technique: Correlation between Nozzle Velocity and Vibration Level of Hydro-Turbine in SHP Run-off-River Scheme

A.Z Jamil, J.Othman, E.A. Azrulhisham

Abstract: ***Regression Examination is one of the most popular statistical analysis method used to determine the correlation between examined variables. It can also be used to predict the value of a dependent variable based on the value of at least one independent variable and this will allow explaining the impact of changes in an independent variable on the dependent variable. With the measured data of flow rate, output power and efficiency of turbine system, the nozzle velocity can be calculated using an appropriate mathematical equation. Along with vibration level data at every measurement axes, they are tabulated and imported into MATLAB program for the correlation determination. Three different set of data are used in this analysis which is based on the variation of water level at different month (low, typical and high) due to rainfall distribution within one year period. The objective of this study was to examine two questions: first is the effect of water level to the measured flow rate and generated output as well the calculated nozzle velocity. Second, with these variation of nozzle velocity, how significance their correlation with the vibration level at multiple axes of the turbine and generator? From the results, it has been discovered that there are significant correlation between nozzle velocity and vibration level, particularly during low level of water (lower rainfall distribution).***

Index Terms: ***Regression Examination, Nozzle Velocity, Vibration Velocity, Correlation***

I. INTRODUCTION

The typical run-off-the-river scheme consists of fundamental elements such as the weir, the settling tank, penstock and small canal [1][2]. Before entering the turbine, the particulate matter is removed by passing water through a settling tank. In order to ensure the unwanted particulate matter is not flowing together with the water source, they will be settling out at the settling tank.

Revised Manuscript Received on August 30, 2019.
* Correspondence Author
AZ Jamil*, Universiti Kuala Lumpur, Malaysia France Institute, Section 14, Jalan Teras Jernang, Bandar Baru Bangi, Selangor, Malaysia.
J.Othman, Universiti Kuala Lumpur, Malaysia France Institute, Section 14, Jalan Teras Jernang, Bandar Baru Bangi, Selangor, Malaysia.
E.A. Azrulhisham, Universiti Kuala Lumpur, Malaysia France Institute, Section 14, Jalan Teras Jernang, Bandar Baru Bangi, Selangor, Malaysia.

As to prevent damage from big sizes of materials such as stones, timber, leaves and man-made litter, the trash rack is located close to the fore-bay. The water is then transported from the fore-bay to the turbine via penstock [3]. The concept of run-off-river scheme as illustrated in Fig. 1.0.

Fig. 1.0The Concept of Run-Off-River [3]

Regression examination is a reliable method of identifying which variables have impact on a topic of interest. The process of performing a regression allows to confidently determining which factors matter most, which factors can be ignored, and how these factors influence each other. The essential components related to this analysis are: i) Dependent Variable: This is the main factor to understand or predict. ii) Independent Variables: These are the factors that are hypothesized to have an impact on the dependent variable. In order to show the relationships between two variables, the scatter plot/scatter diagram is used [4]. The correlation analysis is used to measure strength of the association (linear relationship) between two variables. This analysis is only concerned with strength of the relationship and no causal effect is implied [5] Since there is only one independent variable in this analysis, which is nozzle velocity, the model will be a simple linear regression model. The equation of this linear regression model is given in (1),

$$y = \beta_0 + \beta_1 x + \varepsilon \qquad (1)$$

Whereby *y* is dependent or study variable, *x* is independent or explanatory variable. β_0 is known as intercept term and β_1 is the slope parameter and they are regression coefficients. The unobservable error component ε accounts for the failure of data to lie on the straight line and represents the difference between the true and observed realization of y.

It is assumed that this component as independent and identically distributed random variable with mean zero and constant variance.[6][7]

At Sg Perting Small Hydro Plant, the Turgo turbines are utilized. These are an impulse type of turbine, capable of handling much higher of flow rates as compared to a Pelton turbine.

Because of this feature, the Turgo turbine is much more preferred to be used in hydroelectric plants that require medium hydraulic heads [8]. Fig. 2.0 shows the internal structure of the Turgo turbine.

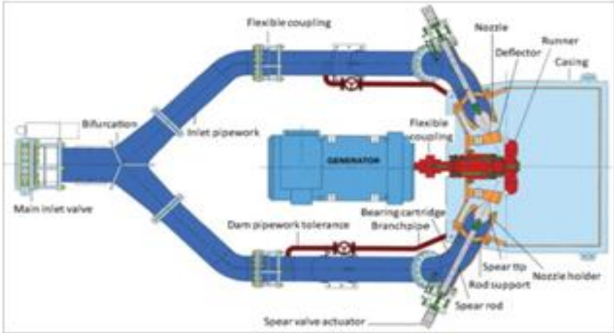

Fig. 2.0 Internal structure of Turgo Turbine

There are nozzles that are properly located for the waterjet to smash the turbine buckets on one side at the angle of about 20°. This waterjet will generate the high speed of water that is appeared surrounding the turbine.[3] This shallow angle allows the water stream to exit on the other side instead of being diverted backwards [3]. Fig. 3.0 illustrates how the nozzle injects the water to the turbine vane.

Fig. 3.0 (a) Nozzle sprays water to the vane

The condition of running turbine's blade operated in the month of March 2017 is shown in Fig. 3.0 (b) below:

Fig 3.0 (b) Turbine's blade before replacement

During the plant shutdown and maintenance in June 2017, the new turbine has been replaced as shown in Fig. 3.0 (c).

Fig. 3.0 (c) Turbine blade after replacement

II. METHODOLOGY

A. Measurement of Water Flow ((Flow rate)

The measurement of water flow is carried out at the intake of hydropower system. Two ultrasonic sensors are installed at each section of settling basin at this intake. This TIENET 310 Ultrasonic Level Sensor [9] is connected to the Signature Flow Meter [10] that is specifically designed for open channel flow monitoring application. The data captured from the level sensor represents the numerical values of flow rates which to be processed by this Signature flow meter [11]. Fig. 4.0 and Fig. 5.0 show the sensor and signature flow meter respectively.

Fig. 4.0 TIENET Ultrasonic Sensor

Fig. 5.0 The Signature Flow Meter

B. Measurement of Output Power (KW)

The generated output power for each generator is recorded and displayed by the power management meter. This meter is located in the Control Room at the powerhouse of hydropower station. Fig. 6.0 shows the Power Management meter.

Fig. 6.0 The Power Management Meter

C. Measurement of Vibration Velocity

For the purpose of statistical analysis, the data of vibration is collected for the duration of fifteen days in three different months with three conditions; one month with average rainfall distribution (March), one month with the lowest rainfall distribution (June) and one month with the highest rainfall distribution (October). The measurement axes at the turbine and generator are as in the Fig. 7.0(a)-(b) respectively.

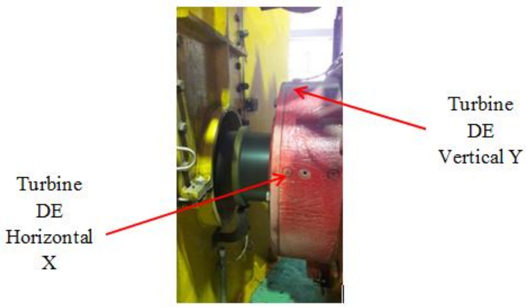

(a) At turbine Driving End (DE)

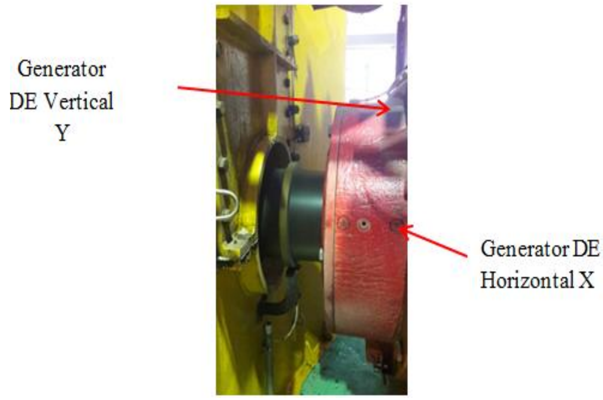

(b) At Generator Driving End (DE)

Fig. 7.0 Measurement Axes of Vibration Velocity

Measurement of vibration velocity is carried out by using VIBSCANNER Analyser as shown in Fig. 8.0 below.

Fig. 8.0 VIBSCANNER Data Collector and Analyser [12]

D. Applied mathematical equation

The relationship between generated output power and flow rate in hydropower system is indicated by (2), in which ρ (kg/m3) represents a density 1000 kg/m3, g(m/s2) represents the acceleration due to gravity 9.81 m/s2, Q (m3/s) denotes the flow rate, and H (m) will be the net head available at the inlet to the turbine, and η is the overall energy conversion efficiency.

$$P=\rho g H Q \eta \quad (2)$$

The kinetic energy $1/2mv^2$ of the water impacting on the blades is the maximum power output from a turbine that is used in a run of river application. Taking into consideration the efficiency η of the turbine and its installation, the maximum output power *Pmax* can be calculated as in (3) in which *v* will be the velocity of the water flow and *Q* represents the volume of water flowing through the turbine per second. Because of there is generator losses in the transformer, the general efficiency for small hydropower system electricity generation is lower (< 80%) than for mechanical power supply system [10],

$$P_{max} = {}^{1}/_{2}\, \eta \rho Q v^2 \quad (3)$$

By manipulating (3), the velocity of water flow into the spear valve (nozzle velocity) can be determined as in (4)

$$v = \sqrt{\frac{2P_{max}}{\eta\rho Q}} \quad (4)$$

E. The characteristic of vibration velocity data distribution.

A box plot or boxplot is a method for graphically depicting groups of numerical data through their quartiles. This will enable to study the distributional characteristics of a group data set as well as the level of the data. Prior to the development of box plot, the statistic parameters such as mean, median, min and max as well as standard deviation are determined [13]

III. RESULTS

A. The sample of data measurement

Table 1.0 (a) – (d) shows the sample result of flow rate, generated output, vibration velocity measurement and calculated nozzle velocity respectively.

Table 1.0 Sample of data measurement

a. Sample measurement of flow rate

Label	Flow Rate	Flow Rate
Units	m3m	m3s
3/1/2017 9:00	186.220337	3.103672283
3/1/2017 10:00	186.66832	3.111138667
3/1/2017 11:00	191.036133	3.18393555
3/1/2017 12:00	203.558533	3.392642217
3/1/2017 13:00	195.240448	3.254007467
3/1/2017 14:00	187.264755	3.12107925
3/1/2017 15:00	187.147964	3.119132733

b. Sample measurement of Output power

Label	Nozzle
Units	Pmax
3/1/2017 9:00	1111.00
3/1/2017 10:00	1111.00
3/1/2017 11:00	1111.00
3/1/2017 12:00	1111.00
3/1/2017 13:00	1111.00
3/1/2017 14:00	1111.00
3/1/2017 15:00	1167.00
3/1/2017 16:00	1167.00
3/1/2017 17:00	1167.00

c. Sample measurement of Vibration Velocity

Label	Turbine				Generator			
Units	SX	SY	B1X	B1Y	B2X	B2Y	B3X	B3Y
3/1/2017 9:00	6.20	4.10	4.20	10.80	6.50	11.30	3.30	8.80
3/1/2017 10:00	6.20	4.10	4.40	12.90	6.20	10.20	3.40	9.20
3/1/2017 11:00	6.40	4.40	4.20	11.80	6.30	10.80	3.60	10.50
3/1/2017 12:00	6.20	3.90	4.40	12.60	6.50	11.40	3.30	9.30
3/1/2017 13:00	6.30	4.30	4.20	12.80	6.50	11.20	3.30	9.20
3/1/2017 14:00	6.30	4.30	4.40	13.20	6.60	11.90	3.40	9.60
3/1/2017 15:00	6.10	4.00	4.30	13.00	6.50	11.60	3.50	9.70
3/1/2017 16:00	6.30	4.40	4.40	13.20	6.40	11.10	3.60	10.20

d. Sample calculated of nozzle velocity

Label	Flow Rate	Nozzle	
Units	m3s	Pmax	Vel
3/1/2017 9:00	3.60	1111.00	16.35072
3/1/2017 10:00	3.61	1111.00	16.31691
3/1/2017 11:00	3.68	1111.00	15.99448
3/1/2017 12:00	3.89	1111.00	15.13692
3/1/2017 13:00	3.75	1111.00	15.69592
3/1/2017 14:00	3.62	1111.00	16.27212
3/1/2017 15:00	3.62	1167.00	16.68614
3/1/2017 16:00	3.57	1167.00	16.90675

For the purpose of the Regression Analysis using MATLAB, data at each measurement axis of vibration velocity is arranged side-by-side with the calculated nozzle velocity. These arrays will be imported into the MATLAB environment for analysis purpose. The sample of this array arrangement is shown in Table 2.0

Table 2.0 Sample of array arrangement

Velocity	Vibration B1X
16.35072	4.05
16.31691	4.14
15.99448	4.02
15.13692	4.07

B. The distributional characteristic of vibration velocity

i. For the month of March 2017

Table 3.0 (a) and (b) represent statistical parameter and the characteristic of box plot of data respectively. Fig. 9.0 shows the box plot.

Table 3.0 (a) Statistical parameter of data

	B1X	B1Y	B2X	B2Y
Count	164	164	164	164
Mean	3.994614	8.712592	3.83628	8.675788
SD	0.411899	1.673787	0.493751	1.778205
Max	4.886934	12.90506	4.893453	12.1052
Q3	4.337459	10.00385	4.227191	10.05926
Median	4.03139	9.004872	3.813816	8.792165
Q1	3.793473	7.21471	3.506069	7.665882
Min	2.649259	4.825299	2.541964	4.013244

Table 3.0 (b) The characteristic of box plot

	B1X	B1Y	B2X	B2Y
Bottom	3.793473	7.21471	3.506069	7.665882
2 Q Box	0.237916	1.790162	0.307747	1.126282
3 Q Box	0.306069	0.998976	0.413375	1.267093
Whisker -	1.144215	2.389411	0.964105	3.652638
Whisker +	0.549475	2.901208	0.666261	2.045944

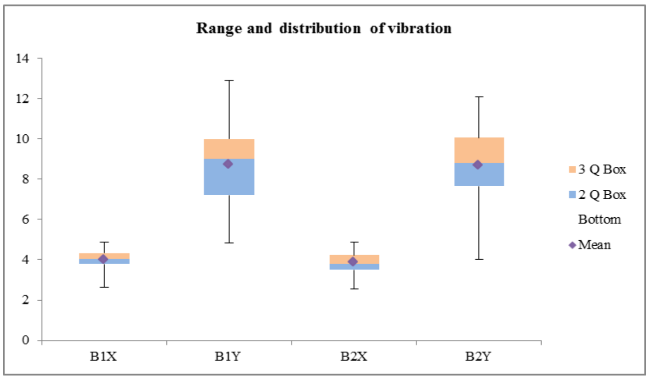

Fig. 9.0 The Box Plot

ii. For the month of June 2017

Table 4.0 (a) and (b) represent statistical parameter and the characteristic of box plot of data respectively. Fig. 10.0 shows the box plot.

Table 4.0 (a) Statistical parameter of data

	B1X	B1Y	B2X	B2Y
Count	159	159	159	159
Mean	2.890252	4.155031	2.566783	4.065409
SD	0.403459	0.435942	0.371663	0.486453
Max	4.290353	5.022535	3.761977	5.00568
Q3	3.14279	4.48505	2.821122	4.252787
Median	2.927336	4.215855	2.604299	4.138029
Q1	2.618524	3.874608	2.297595	3.90472
Min	2.063125	2.736963	1.754856	2.097928

Table 4.0 (b) The characteristic of box plot

	B1X	B1Y	B2X	B2Y
Bottom	2.618524	3.874608	2.297595	3.90472
2 Q Box	0.308812	0.341247	0.306704	0.233309
3 Q Box	0.215454	0.269195	0.216823	0.114758
Whisker -	0.555399	1.137645	0.542739	1.806792
Whisker +	1.147563	0.537486	0.940855	0.752893

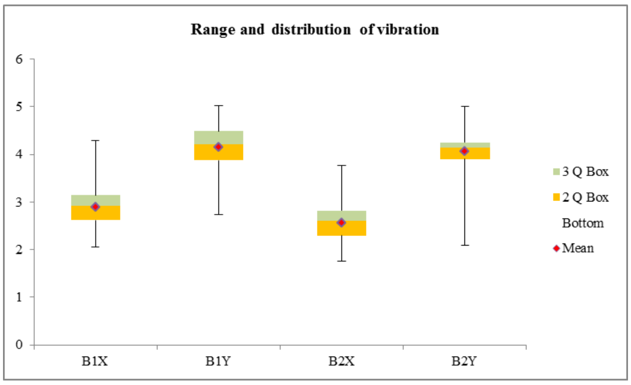

Fig. 10.0 the Box Plot

iii. For the month of October 2017

Table 5.0 (a) and (b) represent statistical parameter and the characteristic of box plot of data respectively. Fig. 11.0 shows the box plot.

Table 5.0 (a) Statistical parameter of data

	B1X	B1Y	B2X	B2Y
Count	154	154	154	154
Mean	2.882143	2.874675	2.747727	2.772727
SD	0.362151	0.302292	0.263511	0.242977
Max	3.971367	3.643184	3.433774	3.39679
Q3	3.063866	3.098859	2.955558	2.943139
Median	2.81664	2.841363	2.759428	2.800946
Q1	2.643174	2.677846	2.55174	2.588005
Min	2.222092	2.110645	2.211069	2.073192

Table 5.0 (b) The characteristic of box plot

	B1X	B1Y	B2X	B2Y
Bottom	2.643174	2.677846	2.55174	2.588005
2 Q Box	0.173467	0.163517	0.207688	0.212941
3 Q Box	0.247225	0.257496	0.19613	0.142193
Whisker -	0.421082	0.567201	0.340671	0.514813
Whisker +	0.907502	0.544325	0.478216	0.453651

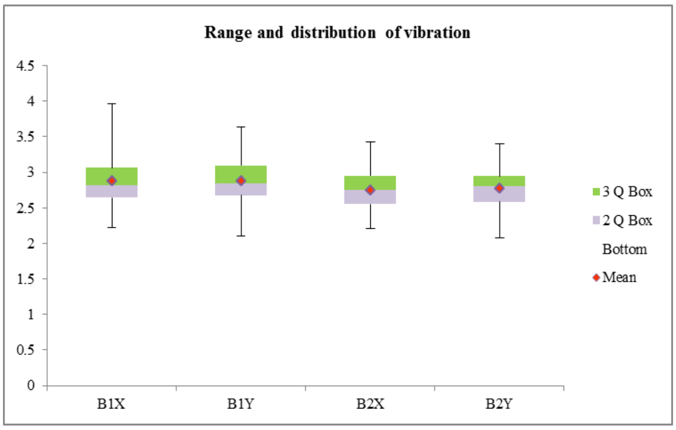

Fig. 11.0 The Box Plot

C. The results of Regression Analysis

The tabulated data of nozzle velocity and vibration velocity for all measurement axes in each month have been imported into MATLAB Curvefit Tools for regression analysis purpose. The scatter plots and regression parameters generated are presented as the following:

i. For the month of March 2017

Fig. 12.0 (a) to (h) represent scatter plot and regression analysis parameter for all axes of vibration measurement points

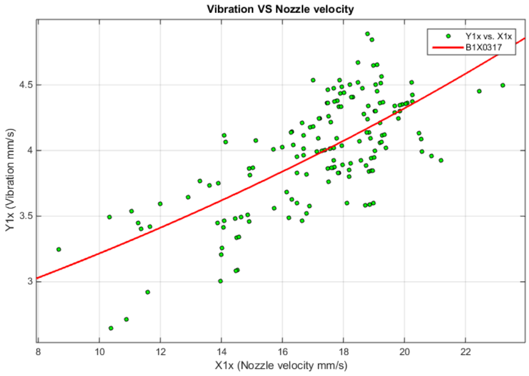

(a) Scatter Plot for B1X

Results

General model Exp1:
f(x) = a*exp(b*x)
Coefficients (with 95% confidence bounds):
a = 2.394 (2.183, 2.605)
b = 0.02954 (0.02457, 0.03451)

Goodness of fit:
SSE: 14.35
R-square: 0.4811
Adjusted R-square: 0.4779
RMSE: 0.2976

(b) Regression analysis parameter

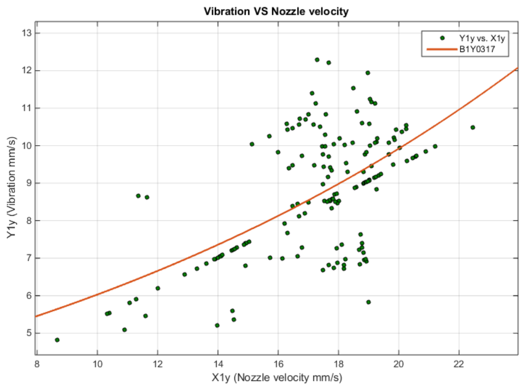

(c) Scatter Plot for B1Y

Results

General model Exp1:
f(x) = a*exp(b*x)
Coefficients (with 95% confidence bounds):
a = 3.666 (2.973, 4.358)
b = 0.04979 (0.03925, 0.06033)

Goodness of fit:
SSE: 283.1
R-square: 0.38
Adjusted R-square: 0.3762
RMSE: 1.322

(d) Regression analysis parameter

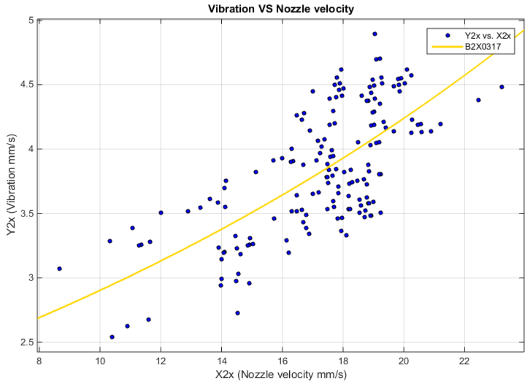

(e) Scatter Plot for B2X

Results

General model Exp1:
f(x) = a*exp(b*x)
Coefficients (with 95% confidence bounds):
a = 1.988 (1.766, 2.209)
b = 0.03788 (0.03162, 0.04414)

Goodness of fit:
SSE: 20.3
R-square: 0.4892
Adjusted R-square: 0.4861
RMSE: 0.354

(f) Regression analysis parameter

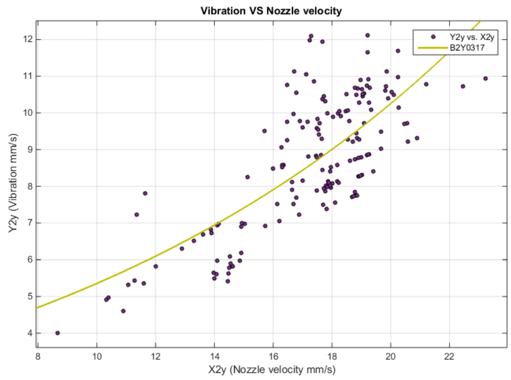

(g) Scatter Plot for B2Y

Results

General model Exp1:
f(x) = a*exp(b*x)
Coefficients (with 95% confidence bounds):
a = 2.796 (2.308, 3.284)
b = 0.06498 (0.05531, 0.07464)

Goodness of fit:
SSE: 223.8
R-square: 0.5658
Adjusted R-square: 0.5631
RMSE: 1.175

(h) Regression analysis parameter

Fig. 12.0 Scatter plot and regression analysis parameter for all axes

The summary of overall Regression Analysis key features is as in Table 6.0 below.

Table 6.0 The overall summary of Regression Analysis parameter

Key Features	Turbine		Generator	
	B1X	B1Y	B2X	B2Y
Correlation	Positive	Positive	Positive	Positive
Null Hyphotheses, H_0:β_1=0	Reject	Reject	Reject	Reject
% Variation of DV by IV	48.11%	38.00%	48.92%	56.58%
p-value (larger or smaller than CI)	smaller	smaller	smaller	smaller
Confidence interval for the slope	not include 0	not include 0	not include	not include 0

ii. For the month of June 2017

Fig. 13.0 (a) to (h) represent scatter plot and regression analysis parameter for all axes of vibration measurement points

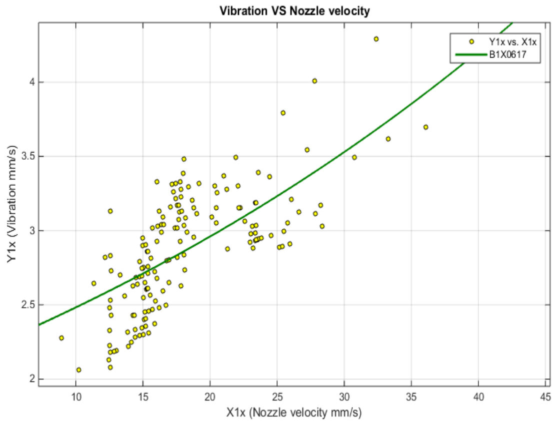

(a) Scatter plot for B1X

Results

General model Exp1:
f(x) = a*exp(b*x)
Coefficients (with 95% confidence bounds):
a = 2.083 (1.976, 2.19)
b = 0.01758 (0.01506, 0.0201)

Goodness of fit:
SSE: 12.37
R-square: 0.5189
Adjusted R-square: 0.5158
RMSE: 0.2807

(b) Regression analysis parameter

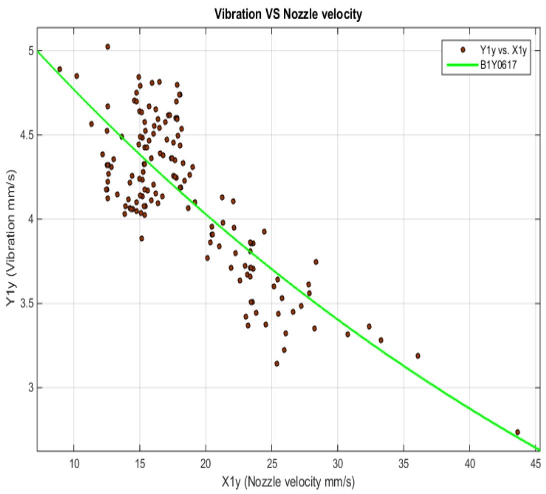

(c) Scatter plot for B1Y

Results

General model Exp1:
f(x) = a*exp(b*x)
Coefficients (with 95% confidence bounds):
a = 5.645 (5.424, 5.867)
b = -0.01686 (-0.01902, -0.0147)

Goodness of fit:
SSE: 11.02
R-square: 0.6328
Adjusted R-square: 0.6305
RMSE: 0.265

(d) Regression analysis parameter

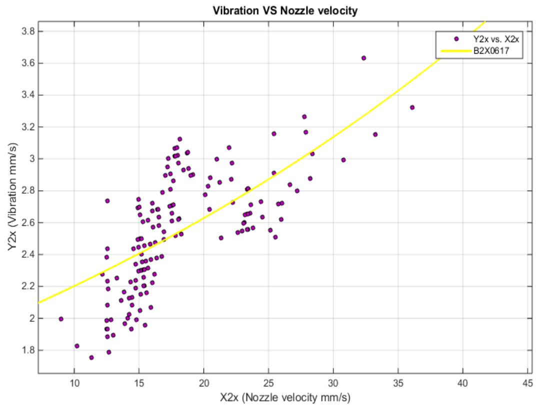

(e) Scatter plot for B2X

Results

General model Exp1:
f(x) = a*exp(b*x)
Coefficients (with 95% confidence bounds):
a = 1.846 (1.745, 1.947)
b = 0.01769 (0.01501, 0.02037)

Goodness of fit:
SSE: 11.06
R-square: 0.4932
Adjusted R-square: 0.4899
RMSE: 0.2654

(f) Regression analysis parameter

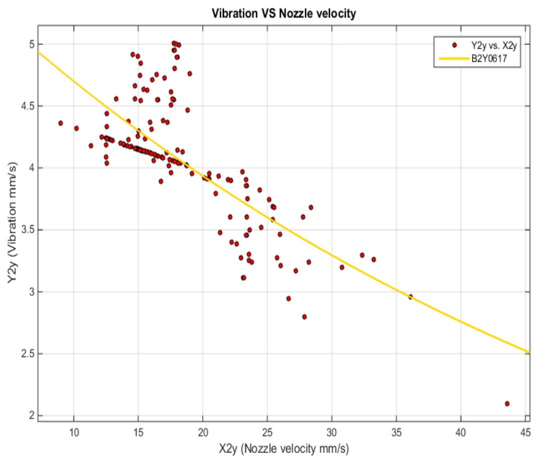

(g) Scatter plot for B2Y

Results

General model Exp1:
f(x) = a*exp(b*x)
Coefficients (with 95% confidence bounds):
a = 5.615 (5.336, 5.894)
b = -0.01777 (-0.02051, -0.01503)

Goodness of fit:
SSE: 16.81
R-square: 0.5503
Adjusted R-square: 0.5474
RMSE: 0.3273

(h) Regression analysis parameter

Fig. 13.0 Scatter plot and regression analysis parameter for all axes

The summary of overall Regression Analysis key features as in Table 7.0 below.

Table 7.0 The overall summary of Regression Analysis parameter

Key Features	Turbine		Generator	
	B1X	B1Y	B2X	B2Y
Correlation	Positive	Positive	Positive	Positive
Null Hyphotheses, H_0:β_1=0	Reject	Reject	Reject	Reject
% Variation of DV by IV	51.89%	63.28%	49.32%	55.03%
p-value (larger or smaller than CI)	smaller	smaller	smaller	smaller
Confidence interval for the slope	not include 0	not include 0	not include	not include 0

iii. For the month of October 2017

Fig. 14.0 (a) to (h) represent scatter plot and regression analysis parameter for all axes of vibration measurement points

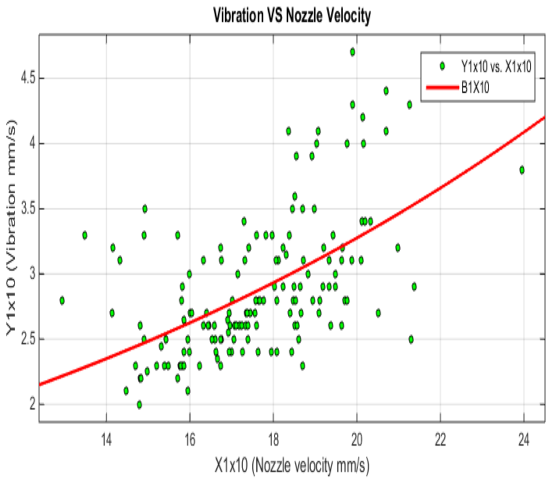

(a) Scatter plot for B1X

Results

General model Exp1:
f(x) = a*exp(b*x)
Coefficients (with 95% confidence bounds):
a = 1.084 (0.8276, 1.34)
b = 0.0553 (0.0422, 0.0684)

Goodness of fit:
SSE: 29.74
R-square: 0.3034
Adjusted R-square: 0.2988
RMSE: 0.4424

(b) Regression analysis parameter

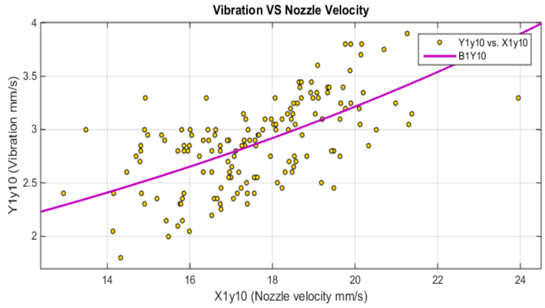

(c) Scatter plot for B1Y

Results

General model Exp1:
f(x) = a*exp(b*x)
Coefficients (with 95% confidence bounds):
a = 1.229 (1.013, 1.444)
b = 0.0481 (0.03836, 0.05783)

Goodness of fit:
SSE: 16.21
R-square: 0.3808
Adjusted R-square: 0.3767
RMSE: 0.3266

(d) Regression analysis parameter

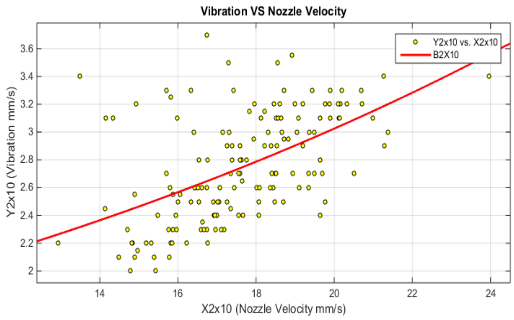

(e) Scatter plot for B2X

Results

General model Exp1:
f(x) = a*exp(b*x)
Coefficients (with 95% confidence bounds):
a = 1.332 (1.087, 1.577)
b = 0.04101 (0.03076, 0.05126)

Goodness of fit:
SSE: 16.31
R-square: 0.2875
Adjusted R-square: 0.2828
RMSE: 0.3275

(f) Regression analysis parameter

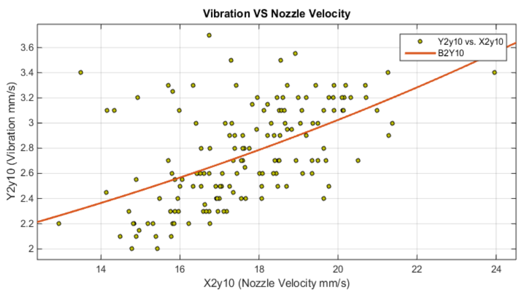

(g) Scatter plot for B2Y

```
Results

General model Exp1:
    f(x) = a*exp(b*x)
Coefficients (with 95% confidence bounds):
    a =     1.332  (1.087, 1.577)
    b =   0.04101  (0.03076, 0.05126)

Goodness of fit:
  SSE: 16.31
  R-square: 0.2875
  Adjusted R-square: 0.2828
  RMSE: 0.3275
```

(h) Regression analysis parameter

Fig. 14.0 Scatter plot and regression analysis parameter for all axes

The summary of overall Regression Analysis key features as in Table 8.0 below.

Table 8.0 The overall summary of Regression Analysis parameter.

Key Features	Turbine		Generator	
	B1X	B1Y	B2X	B2Y
Correlation	Positive	Positive	Positive	Positive
Null Hyphotheses, H_0:β_1=0	Reject	Reject	Reject	Reject
% Variation of DV by IV	30.34%	38.08%	28.75%	28.75%
p-value (larger or smaller than CI)	smaller	smaller	smaller	smaller
Confidence interval for the slope	not include 0	not include 0	not include	not include 0

IV. DISCUSSIONS

From the results of the box plot, it can be seen that in a month of March, given the much longer whiskers in B1Y and B2Y, they vary more widely in terms of vibration velocity measured at that two axes compared to B1X and B2X.

In the month of June, the similar characteristic obviously can be identified at the B2Y axis, but the other axes seem to have evenly length of whisker.

In contrast to the characteristic of box plot in October, all axes exhibit quite similar length of whisker.

With regards to the regression analysis results, particularly related to the coefficient of determination, R^2 it can be observed that in the month of March, the percentage of correlation between dependent variable (vibration velocity) and independent variable (nozzle velocity) lie in the range of 48% to 58%, with the highest occur at the B2Y axis.

In the month of June, the percentage variation of dependent variable and independent variable in the range of 50% to 63% with the highest recorded at B1Y and B2Y respectively.

Meanwhile, in the month of October, much smaller correlation is notified, with the range from 29% to 38%, with the highest can be seen at B1Y axis.

In all cases, the 95% confidence interval does not include 0, which mean that there is significant relationship between vibration velocity and nozzle velocity.

V. CONCLUSION

a. Related to the distribution characteristics of measured vibration velocity data represented in box plot;

- The highest vibration velocity is recorded in the month of March 2017 affected by some broken blade on the turbine.
- The significantly reduced of vibration velocity measured in the month of June and October 2017 after the damaged turbine has been replaced with a new one.
- The percentage of spear valve opening has also influenced the level vibration velocity in order to maintain the rotational speed of turbine at 750 rpm. During the low level water operation (in June 2017), valve is opened up to 100% and the data recorded is slightly higher. At high level water operation (in October 2017), valve is adjusted not more than 50% opening, the vibration velocity data is slightly similar as in the case of June 2017.
- In March 2017, with some damages on the blade, the valve is kept opened not more than 50% (due to avoid high level noise developed) but still recorded high vibration velocity.

b. With regards to the regression analysis results presented in scatter plot and table goodness of fit:

- The most significant correlation between vibration velocity and nozzle velocity can be observed in the month of June. This is contributed by the large percentage of spear valve opening in order to allow sufficient volume of water to drive the turbine as to maintain the rotational speed of the turbine. Because of the volume is increased, the nozzle velocity is higher, initiated vibration velocity at driving end of turbine, propagated into other component in the system.
- Similar outcome can be seen in the month of October. However because the water level is high, spear valve is adjusted in a much lower percentage so that the volume of water is enough to drive and maintain the speed of turbine. Because of the nozzle velocity is significantly high, the vibration velocity is developed and distributed to other connected components in the system

ACKNOWLEDGMENT

This paper is part of PhD research works on “Condition Monitoring and Predictive Maintenance System for Run-Off-River Hydropower Plant” which is supported by Amcorp Perting Hydro Sdn. Bhd. This project is partly funded by the Ministry of Energy, Green Technology and Water; KeTTHA_AAIBE Research Grant 02-1-56-1565.

REFERENCES

1. K. Okot, “Review of small hydropower technology,” Renew. Sustain. Energy Rev., vol. 26, pp. 515–520, 2013.
2. UNIDO and International Center on Small Hydro power, “World Small Hydropower Development Report 2016,” Int. Netw. Small Hydro Power, 2016.
3. H. Ramos, “Guidelines for design of small hydropower plants,” Guidel. Des. small hydropower plants, p. 210, 1999.
4. Strasheim, “Basic Statistical Analysis in Research,” 2016.
5. R. kumar and S. K. Singal, “Operation and Maintenance Problems in Hydro Turbine Material in Small Hydro Power Plant,” Mater. Today Proc., vol. 2, no. 4–5, pp. 2323–2331, 2015.
6. R. Analysis, “Chapter 2 Simple Linear Regression Analysis The simple linear regression model,” pp. 1–42, 2019.

7. L. Edwards, "The correlation coefficient. An introduction to linear regression and correlation," Correl. Coeff. An Introd. to Linear Regres. Correl. Chap 4, pp. 33–46, 1976.
8. O. Paish, "Small hydro power: Technology and current status," Renew. Sustain. Energy Rev., vol. 6, no. 6, pp. 537–556, 2002.
9. T. Isco, "TIENet ® 310 Ultrasonic," no. May, 2015.
10. S. Features, "A highly flexible monitoring platform, adapting right along with your current need and any future changes in your monitoring requirements."
11. X. Uxoklvkdp, D. P. Dql, D. Q. Egxoodk, and D. Dqgx, "GSM Wireless Datalogger of Small Hydro Power Generation System," pp. 246–251, 2014.
12. Schritte, "OMNITREND ® Web," 2012.
13. V. Box and W. Plots, "Vertical Box and Whisker Plots," Atlantic, pp. 1–6, 2008.
14. Harvey, A. Brown, P. Hettiarachi and A. Inversion, "Micro-Hydro Design Manual: A guide to small-scale water power schemes," Practical Action Publishing, ISBN: 978-1-85339-103-3, 1993.
15. M.F. Basar, A. Ahmad, N. Hasim and K. Sopian, "Introduction to the Pico Hydro Power and the Status of Implementation in Malaysia", IEEE Student Conference on Research and Development, 2011.
16. "World Small Hydropower Development Report 2013," www.smallhydropowerworld.org, 2013
17. "Final Report Renewable Energy Technology Roadmap," Malaysia Industry Government Group for High Technology, 2010.
18. "Malaysia Report on Small Hydro Power (SHP)," Malaysia Industry Government Group for High Technology, 2012.
19. http://energyeducation.ca/encyclopedia/Turgo_turbine

AUTHORS PROFILE

A.Z Jamil is currently completing his PhD studies in Electrical & Engineering, focusing on Condition Monitoring and Predictive Maintenance System. He has obtained his Master in Control System Engineering from University of Sheffield in 2007. His research interest is in the area of condition monitoring and has published several papers related to that topic.

J.Othman is a Professor at University Kuala Lumpur Malaysia France Institute. He has obtained his Bachelor Degree in Electrical Engineering from Universite de Nancy, France, Master Degree from University Kebangsaan Malaysia and PhD in Manufacturing Engineering from Dublin City University, Ireland. His research area is in industrial automation and manufacturing, including the area of Condition Monitoring has published several papers related to that topic.

E.A. Azrulhisham is Associate Professor at the Universiti Kuala Lumpur – Malaysia France Institute. Obtained his PhD in Mechanical Engineering from the National University of Malaysia, he is the founder of Sustainable Energy Analysis Laboratory at the Universiti Kuala Lumpur with research interest on development, demonstration and commercialization of renewable energy.